Research Square

Preprints are preliminary reports that have not undergone peer review.
They should not be considered conclusive, used to inform clinical practice,
or referenced by the media as validated information.

Computational Screening of Natural Products Against SOD1 to Identify Potential ALS Therapeutics

Naveed Iqbal
Islamia University of Bahawalpur
Mahmoud Kandeel
King Faisal University
Saba Beigh
Al Baha University
Fatima Rasheed
Islamia University of Bahawalpur
Muhammad Nasir Iqbal
nasir.iqbal@iub.edu.pk
Islamia University of Bahawalpur
Shahid Ullah
S khan lab Mardan KP

Article

Keywords:

Posted Date: March 4th, 2026

DOI: https://doi.org/10.21203/rs.3.rs-8879349/v1

License: This work is licensed under a Creative Commons Attribution 4.0 International License.
Read Full License

Additional Declarations: No competing interests reported.

Computational Screening of Natural Products Against SOD1 to Identify Potential ALS Therapeutics

Naveed Iqbal[1¶], Mahmoud Kandeel[2,3¶], Saba Beigh[4], Fatima Rasheed[1], Muhammad Nasir Iqbal[1*], Shahid Ullah[5*]

[1]Department of Bioinformatics, Institute of Biochemistry, Biotechnology, Bioinformatics, The Islamia University of Bahawalpur, Pakistan.

[2]Department of Biomedical Sciences, College of Veterinary Medicine, King Faisal University, Al-Hofuf, Al-Ahsa, Saudi Arabia.

[3]Department of Pharmacology, Faculty of Veterinary Medicine, Kafrelshikh University, Kafrelshikh, Egypt.

[4]Department of Public Health, College of Applied Medical Science, Al-baha University, Al-Baha 65431, Saudi Arabia.

[5]S khan lab Mardan KP, Pakistan

¶ Equally contributing authors.

* Corresponding authors: nasir.iqbal@iub.edu.pk , drskbioch@gmail.com

Abstract

Neurodegenerative diseases are becoming more common and encompass multiple disorders that result in the loss of neurons, aging of the brain, and eventually lead to death. Amyotrophic lateral sclerosis (ALS) is the most common and devastating neurological disease driven by a gradual loss of motor neurons. It is essential to use cutting-edge technology in drug discovery as conventional methods become slower and more costly. *In silico* strategies provide a reliable, quick, and affordable alternative to the clumsy in vitro methods to improve our understanding of how drugs affect protein structure and related activities. Natural products have strong anti-inflammatory and antioxidant activities. In the present work, we test natural compounds against the SOD1 protein to combat the ALS disease. After identification of the protein, we performed structure-based pharmacophore screening and ADMET analyses of the top hit compounds based on RMSD. Molecular docking and molecular dynamics simulation analyses were applied, and the top two novel compounds reported against ALS showed effective binding properties. The dynamics simulation experiments were conducted at a 100 ns scale to identify the protein's behavior toward the recognized two ligands, Scytonine and Raocyclamide_A. The novel compounds Scytonine and Raocyclamide_A are non-toxic and meet the requirements of ADMET and BBB likeness parameters. The findings from this study will aid researchers in understanding the chemical compounds that interact with our target SOD1 protein. Furthermore, a future path in the realm of drug discovery may involve studying these molecules in vivo/vitro will help to design and test therapeutic medications.

Introduction

The data collected by the World Health Organization insinuates that neurological disorders are salient and widening causes of morbidity. According to the GBD report (Global Burden of Disease), 33% of liver with disability and 13% lived with disability-adjusted years of life with an impairment associated with neurological problems[1, 2]. Unfortunately, the burden of these disorders in developing areas persists mainly in unrecognized neurological disorders that affect the peripheral and central nervous systems[3]. Neurological disorders can be caused by autoimmune-mediated neuron loss, malnutrition, ischemia, numerous mutations, endoplasmic reticulum cell stress, oxidative stress, inflammation, genetic defects, and viral or prion diseases, as well as aberrant protein deposition in brain tissue.[4, 5].

The gradual degradation of motor neurons in the spinal cord, brain, and cortex is a characteristic of amyotrophic lateral sclerosis.[6]. ALS is a fatal neurodegenerative disorder associated with the loss of upper and lower motor neurons in the brain, cortex, and spinal nerve cells respectively.[7] As motor neurons degenerate, they stop the proper functioning of voluntary muscles. As a result, muscles gradually get weakened[8]. Eventually, the brain loses control of voluntary muscle actions[9]. ALS is a diversified disorder with high phenotypic variance. In most patients, the reason for ALS disease is perplexity and case inheritance.[2] ALS can classified as either hereditary or sporadic. Sporadic is a more common type of ALS making up 90-95% of all cases. Familial is a less common type of ALS and 5-10% of cases are thought to be inherited[10]. After diagnosis of ALS, patients do not have more than two to five years. This disease's annual incidence is 2-3 per 100,000 individuals with approximated worldwide lethality of 30,000 patients a year. ALS mostly affects at the age 40 to 70 years but adult patients may be affected[11].

Various genetic and environmental risk factors have been involved in the pathogenesis of ALS disease. Medical analysis based on evidence reveals smoking, chemicals, toxic metals, pesticides, trauma, and neuro-inflammation involved in ALS disease [12, 13]. Mutations in more than twenty genes are common causes of Amyotrophic lateral sclerosis but five genes C9ORF72, FUS, UBQLN2, TARDBP, and SOD1 are the most important identified in ALS cases [14]. Mutations in the Cu/Zn superoxide dismutase-1 gene cause familial ALS. The toxicity of mutation in the SOD1 gene in sporadic ALS is still unclear[15]. These mutations lead to amino acid deletions or insertions [16]. Mutant SOD1 has led to various actions that can relate to its pathophysiology. These include oxidative stress, Endoplasmic reticulum stress, neurotoxicity stress, mitochondrial dysfunction, and axonal transport disruption[17]. Superoxide dismutase-1 mutations lessen protein stability and contribute to aggregation. The protein aggregation and unfolding due to oxidative damage in SOD1 due to mutations [18]. Mutant SOD1 has led to various actions that can relate to its pathophysiology. These aggregates cause oxidative stress, Endoplasmic reticulum stress, neurotoxicity stress, mitochondrial dysfunction, and axonal transport disruption. The mutation in SOD1 causes the failure of antioxidant properties that are the main reason for gaining abnormal toxic activities which lead to cause of ALS disease.

n ALS disease first signs weakness in the limb and develops after a few days, more commonly a few weeks to months later weakness in another limb. Sometimes the initial problem can be one of

dysarthria and dysphagia. The signs and symptoms of ALS spasms and cramping of muscles in hands and arms, disturbance in sleep, constipation, depression and anxiety, emotional lability, sialorrhea, and dyspnea [19-22]. Symptoms may include as the disease progresses, trouble breathing, swallowing and lead to paralysis [23, 24]. The diagnosis of ALS must be handled empathically because it is calamitous for the patients and family members. The diagnosis of ALS can be performed through lab tests, muscle or nerve biopsy, spinal tap, Magnetic resonance imaging, nerve conduction study, and electromyography [25-27].

Drug development is a costly and convoluted process because drugs must carry out some criteria of being innocuous, powerful, and bioavailable[28]. Now, computational and bioinformatics methods accelerate the process of drug discovery which is safe, low-cost, and, streamlined[29]. Bioinformatics approaches can be contrived substantiality for the design and development of novel drugs from natural resources [30, 31]. The inclusive therapeutic potential of various distinctive natural compounds extracted from plants is rich in secondary bioactive metabolites[32]. Natural products are of natural origin, have a fewer side effect and low cost still provide new clinical drugs in anti-infective, neurological diseases, and immunosuppression areas. Natural products are biologically active agents, structural diversity, and strong antioxidants [33]. Natural products are flow resources for discovering potential new drugs[34].

Materials and methods

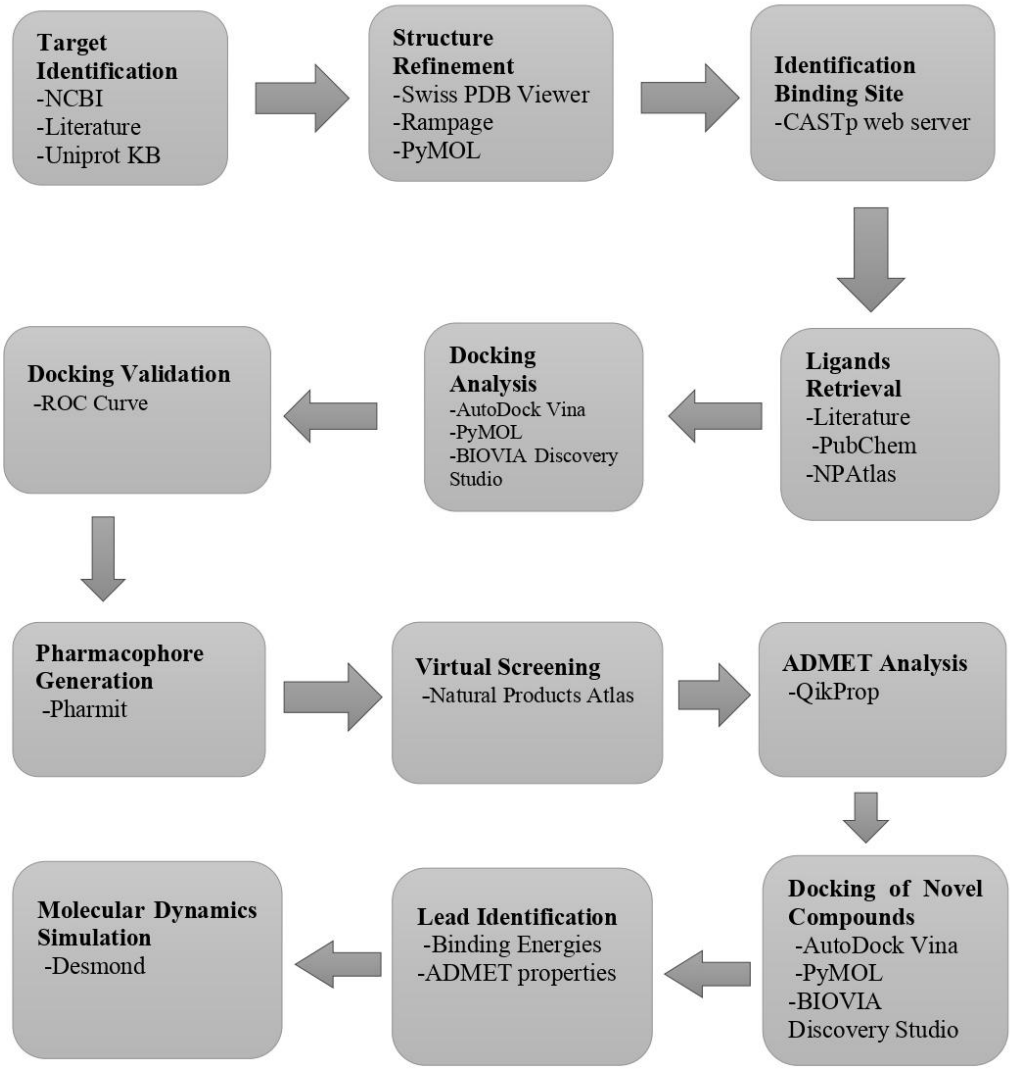


Figure 1: The flowchart that was used to illustrate the methodology process

Protein preparation and compounds database preparation

Figure 1 represents the bird view of methodology adopted for this research along with the tools used. The 3D crystal structure of the SOD1 protein was retrieved from the Protein Data Bank (PDB)[35] having PDB ID: 4A7V as shown in Figure 2 [16]. MODELLER 10.5 was used for loop refinement[36]. RAMPAGE and Swiss PDB Viewer were used for optimization and minimization of the crystal structure of protein[37, 38]. The active binding pocket of protein was identified by the CASTp web server. The CASTp 3.0 version is used for pocket visualization of the target protein[39]. The Natural Products atlas, an inclusive library having natural compounds was selected for pharmacophore-based virtual screening that contains 25,989 small molecules[40].

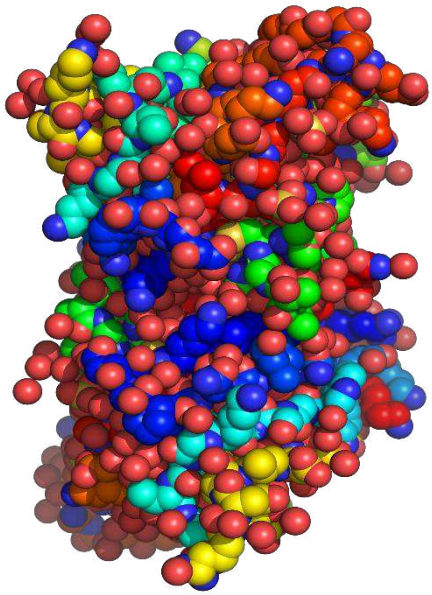


Figure 2:Structure of mutant SOD1 protein (PDB ID: 4A7V) with water molecules, attached ligands and hetatom.

Pharmacophore modeling and virtual screening

The pharmacophore model was generated using the Pharmit online web server[41] (http://pharmit.csb.pitt.edu). The pharmacophore model was prepared based on the selected protein crystallized structure and reported active compounds for our selected target protein by adjusting the 1Å RMSD value. The Pharmacist server provides a framework for the virtual

screening of databases using suitable pharmacophore features, i.e. structural and chemical similarity of compounds that bind actively to our target receptor[42]. For the construction of a coherent pharmacophore query, four main features of ligands hydrogen bonds acceptors, donors, aromaticity, and hydrophobicity were preferred for virtual screening[43]. The pharmacophore query was used to screen the compounds library through the virtual screening process. To identify potential drugs with characteristics or attributes that are compatible with the target site on the covet protein, virtual screening really comprises searching through a sizable library of small molecules[44]. Efficient prioritization and selection of compounds for further exploration may ease researchers in expediting the medication development process. In this specific instance, the natural products atlas were used for screening, which includes drugs that have been approved for use as medicine in the past or are undergoing various stages of study.

Molecular docking analyses and validation

docking to observe the befitting binding orientation of one small molecule to the other receptor to establish a strong stable complex. According to RMSD scores of pharmacophore query in concern to mutant SOD1 protein to make decision of potential inhibitors. The top fifty compound hits were sorted on the base of pharmacophore-fit RMSD score for molecular docking, AutoDock Vina[45] was used and energy dissipated. The dimensions of the grid box were center-x = 1.3739, center-y = -0.2126, center-z = 13.1929, size-x = 51.0131, size-y = 69.2715, and size-z = 51.9292. BIOVIA Discovery Studio examined 2D interactions of protein-ligands and visualized them by PyMol[46].

High throughput virtual screening was performed using the ideal score mechanism to carefully examine the suitable inhibitors. A decoy dataset[47] f active and inactive ligands was used to provoke the highest scoring functions for screening the unknown drugs. To build the decoy dataset, the Enhanced Collection of Valuable Decoys was employed. Docking was performed active and decoys ligands against our target protein. Higher scores for active ligands relative to inactive ligands were determined by using receiver operating characteristic curves (ROC curves) to evaluate the validity of the chosen scoring functions [48]. R language script was used to compute the ROC curve[49].

ADMET analyses

Drug likeness and toxicity analyses of top-ranked compounds were carried out to predict the mutagenicity the carcinogenicity characteristics of selected lead likeness compounds. Schrödinger software package of the QikProp program was used for ADMET[50]. Based on the findings of the ADMET study and the docking binding affinity data, we identified some chemicals having promising features.

Molecular dynamics simulation

The stability of protein-ligand complexes was persuaded by molecular dynamics simulation. Desmond, a package of Schrödinger LLC[51] was used for analyzing molecular dynamics simulation at 100 nanoseconds. Initially, protein-ligand docked complexes apprise binding status in rigid environments [52]. The simulation analysis was performed to check the flexibility of proteins and ligands in the physiological environment[53].

Maestro's Protein Preparation Wizard was employed to optimize and minimize the chosen proteins and ligands. Steric conflicts, inappropriate contacts, and disorganized geometries were fixed during this process. System builder was applied to fabricate the system and solvent model of TIP3P utilized with a force field of OPLS_2005 in the simulation[54]. For neutralization, the counter ions were introduced in the model. To imitate the physiological environment 0.15M amount of sodium chloride with 300k temperature and 1 atm pressure was introduced during the whole period of simulation. Before the simulation, the models were alleviated. Protein and ligand stability were examined by (RMSD) ligand's root mean square deviation during the simulation time[55]. The trajectory was put aside for analysis after every 100-pico seconds (PS).

MM-GBSA: Molecular mechanics and generalized born surface area calculations

The MM-GBSA module in Prime was used to calculate the binding free energies of the docked SOD1 complexes with Scytonine and Raocyclamide_A during molecular dynamics simulation. For free binding energy calculations, the VSGB solvent model, search techniques of rotamer, and OPLS 2005 force field were employed. The frames of MD trajectory after running of simulation at an interim of 10ns.Following equation 1 was utilized to free energy calculations,

$$dGbind = Gcomplex - (Gprotein + Gligand) \qquad (1)$$

Where dGbind = binding free energy, Gligand = free energy of the ligand, Gprotein = free energy of the target protein, and Gcomplex = free energy of the complex.

Results

Data retrieval and preparation

The 3D crystal structure of our target protein SOD1 (4A7V) was retrieved from PDB. The total structural weight is 32.43 kDa. The overall symmetry defined as Cyclic - C2 and Stoichiometry of complex SOD1 is Homo 2-mer - A2. The structure of protein SOD1 was optimized and minimized (Fig. 3) for additional examination. Through this process, protein structure was optimized, appropriate hydrogen atoms added, loop refinement, and suitable bonds assigned for getting the native conformation of our target protein SOD [56, 57]. The active binding pocket of the SOD1 protein was visualized and identified by the CASTp server[39]. The target protein with a binding pocket is shown below in Fig.4.

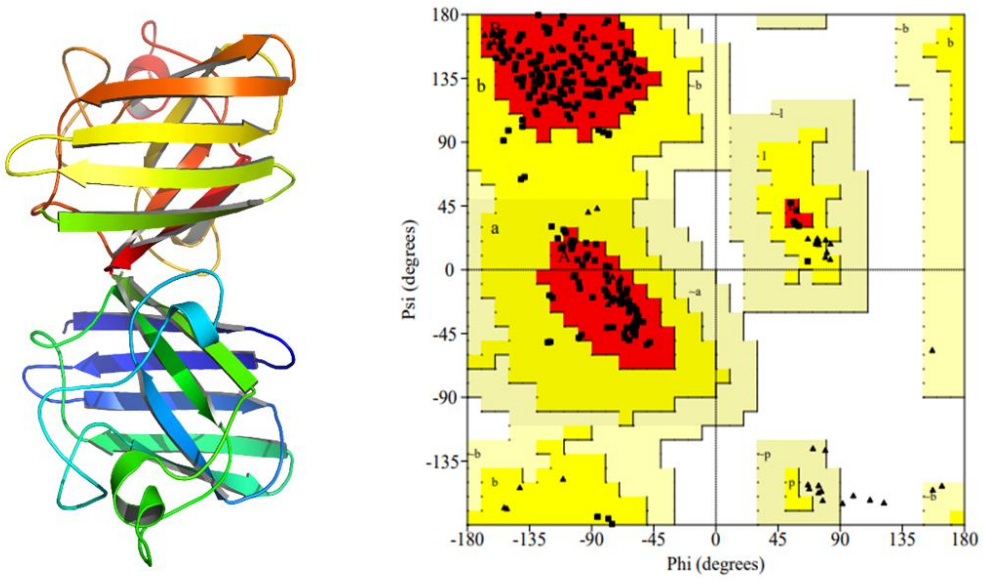


Figure 3: A Ramachandran plot displaying several areas of our target protein's structure was obtained from the PDB along with the protein's 3D crystal structure.

The evaluation of the predicted structure was performed and the overall quality of protein is 91.7 %. Glycine plotted as triangles and proline as squares displayed residue in circles. In the Plot, the yellow area is "allowed", orange is "favored" and the white area is "disallowed regions (Fig. 3)[58]

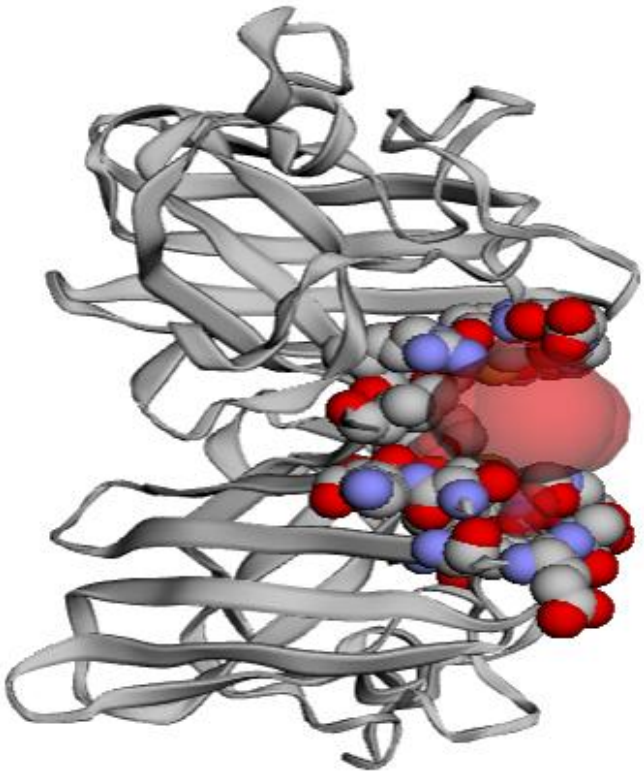


Figure 4: The 3D Structure of SOD1 Protein with binding pocket

Pharmacophore modeling

The pharmacophore query is constructed based on selected common features of pharmacophore characteristics like hydrogen bond acceptors, donors, aromatic rings, and hydrophobicity via the Pharmit online web server. For SOD1, F1, F2, F3, and F4 are pharmacophore characteristics stand (Fig. 5) for Hydrogen bond donor, aromatic ring, hydrogen bond acceptor, and hydrophobicity. The Natural Products Atlas database was used for the screening of compounds via pharmacophore modeling. The top fifty compound hits were sorted on the base of the RMSD score of

pharmacophore features for SOD1 as represented in table 1. Figure 5 illustrates the integrated pharmacophoric feature based on analogous properties.

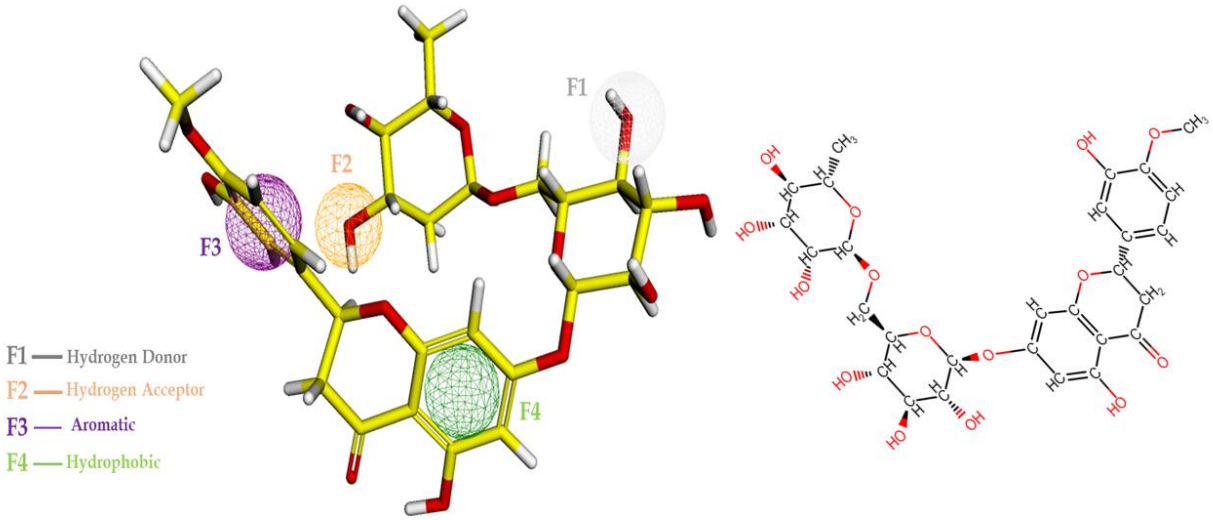
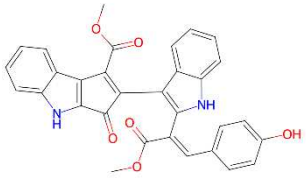
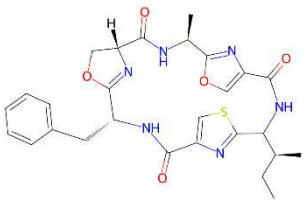
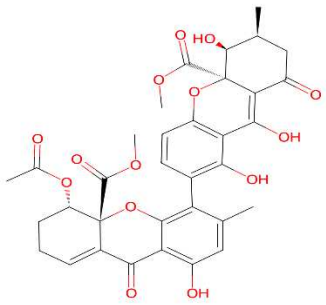
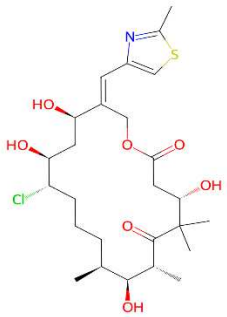
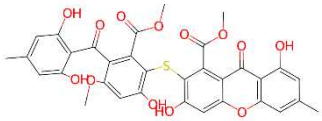


Figure 5: Pharmacophore model and selected ligand fit on pharmacophore hypothesis

Table 1. Pharmacophore score, 3-dimensional structures, id's and names of top compounds

Ligands	NPAID	2D Structures	Pharmacophore RMSD
Scytonine	NPA001113		0.343523
Raocyclamide_A	NPA012630		0.319126

Usneaxanthone_D	NPA027018		0.391716
Epothilone_N	NPA008090		0.40842
Dioschrin	NPA006209		0.356837

Pharmacokinetics and toxicity analysis

The selected natural compounds were rigorously analyzed by assessing the pharmacokinetics and toxicity characteristics of the top fifty ligands. An initial evaluation of the compound's pharmacokinetics and toxicity is essential that aids in selecting an effective therapeutic molecule from all the gathered natural substances. MW, SASA, Donor HB, Accpt_HB, QPlog_HERG, QPP_Caco, QPlog_BB, QPlog_Khsa, QPLog Po/w, and drug-likeliness features of Lipinski Accessibility are among the qualities that have been studied. Due to their noncompliance with regulations and positive toxicity, several substances were left out[59]. The substances' different pharmacokinetic and toxicity characteristics have been evaluated.

Table 2. Showing Pharmacokinetics and toxicity properties of top selected compounds

Molecules	mol_MW	SASA	Donor HB	Accpt HB	QPlog Po/w	QPlog HERG	QPP Caco	QPlog BB	QPlog Khsa
Scytonine	518.5	716.389	0	12	1.006	-6.294	67.414	-2.018	-0.936
Raocyclamide_A	550.6	717.546	0	14.5	0.282	-5.699	108.065	-2.289	-1.951
Usneaxanthone_D	664.6	812.538	0	21	-2.426	-5.479	10.112	-2.843	-2.517
Epothilone_N	546.1	673.863	0	14	0.489	-4.442	223.967	-1.733	-2.02
Dioschrin	662.6	856.868	0	20	-1.667	-5.94	14.911	-3.088	-2.328

Molecular docking analysis

Molecular docking analyses were carried out through Auto Dock Vina for the top hits. All water molecules, ions, and other extra heteroatoms were removed before performing docking analyses. The molecular docking analyses were executed with our prepared target SOD1 protein [60]. The bioinformatics tools have efficient capacity for the selection of compounds and further refinement of selected molecules based on ADMET analyses and docking scores for the identification of potent compounds[61]. In Table 3 the binding affinity and interacting residues are shown. Complete molecular docking results are shown in supplementary file S1.

Table 3: The five lead drugs' molecular docking scores with target protein binding residues

Ligands	PubChem ID	Binding energy (kcal/mol)	Binding Residues
Scytonine	10256051	-8.2	VAL:A_7, LYS:A_9 LYS:F_9, GLY:F_10 ASP:F_11, ASN:F_53 CYS:F_53,ARG:F_143 CYS:F_146
Raocyclamide_A	139586607	-8	THR:A_2, SER:A_107 CYS:A_111, THR:A_118 ILE:A_151, GLY:F_108 CYS:F_111, ARG:F_115 ILF:F_151
Usneaxanthone_D	146683423	-7.5	SER:A_107, GLY:A_108 ARG:A_115, SER:F_107 CYS:F_111, ILE:F_151
Epothilone_N	49780983	-7.4	CYS:A_111, CYS:F_111, THR:A_113
Dioschrin	101888813	-7	LEU:A_106, GLY:A_108 CYS:A_111,THR:A_113 LEU:F_106, ASP:F_109 CYS:F_111, ARG:F_115 ILE:F_151

Protein-ligand interaction analysis

Among the selected compounds, Scytonine and Raocyclamide_A were more effective after thorough molecular docking analyses. Scytonine is a natural product chemically cinnamate ester prevalent in cyanobacteria and scotoma. Scytonine is used as an anti-proliferative and anti-inflammatory drug[62]. Scytonine showed binding affinity -8.2 Kcal/mol with critical binding residues VAL:A_7, LYS:A_9, LYS:F_9, GLY:F_10, ASP:F_11, ASN:F_53, CYS:F_53, ARG:F_143 and CYS:F_146 observed in molecular docking analyses against our target SOD1(Fig.6).

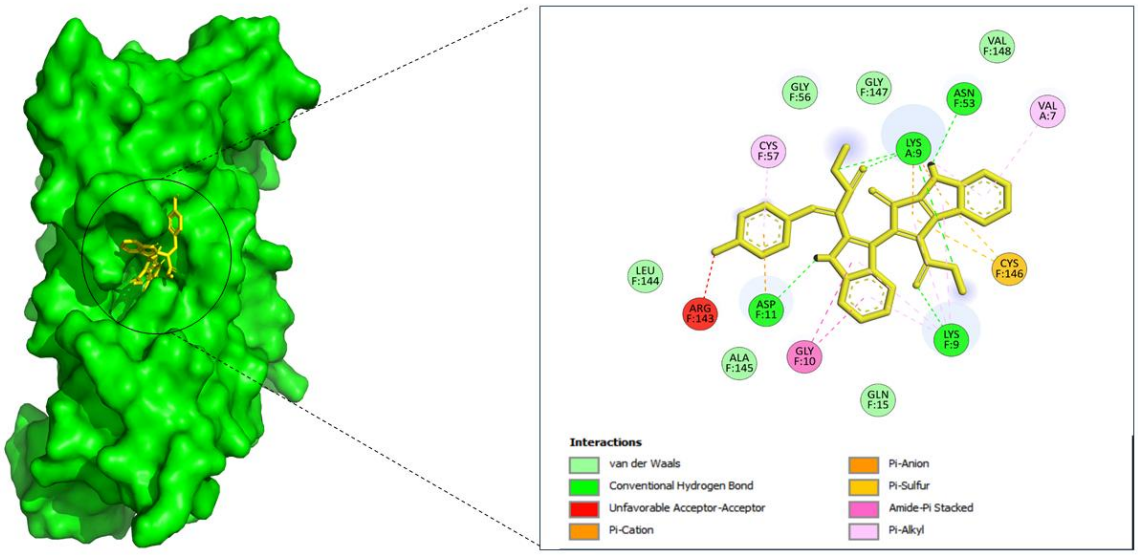


Figure 6: The interaction residues of the Scytonine compound against the SOD1 selected protein.

Raocyclamide_A is a cyclic hexapeptide secondary metabolite prevalent in cyanobacterium Oscillatoria raoi. Raocyclamide_A cyclo-thiazole-d-Ile-oxazole-l-Ala-d-oxazoline-d-Phe and Sea urchin embryos are moderately cytotoxic to Raocyclamide_A[63]. he scrutinized compound Raocyclamide_A showed affective binding interactions and critical binding residues THR:A_2, SER:A_107, CYS:A_111, THR:A_118, ILE:A_151, GLY:F_108, CYS:F_111, ARG:F_115 and ILF:F_151 observed molecular docking analyses against SOD1 our target protein (Fig. 7). Molecular docking investigations along with MD simulations indicated that the identified selected compounds. Scytonine and Raocyclamide_A must satisfy the therapeutic drug characteristics with the lowest binding energy. Scytonine and Raocyclamide_A are thought to be powerful drugs against ALS disease by targeting SOD1 based on the fulfillment of the parameters of ADMET analyses, binding energy, and binding affinity.

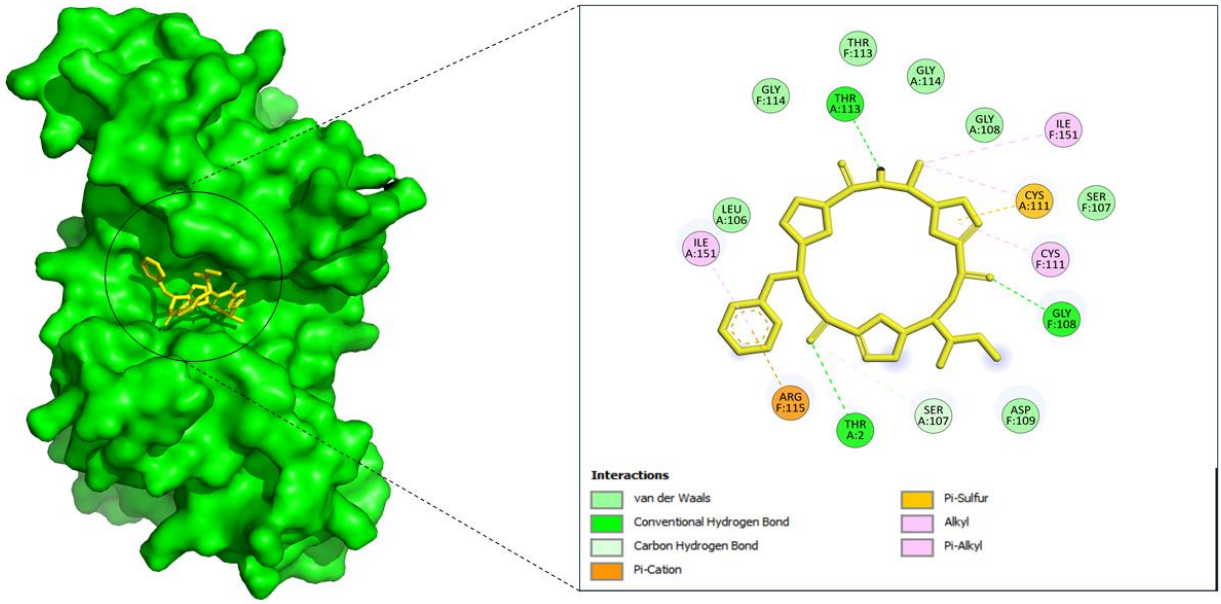


Figure 7: The interaction residues of the Raocyclamide_A compound against the SOD1 selected protein.

Validation of molecular docking

ROC curves were used to create visual representations between test specificity and sensitivity candidates. The percentage of false positives and the proportion of real positives were used to generate the ROC curves. The selection of compounds selected for molecular docking analyses were found to be active ligands rather than inert ligands (decoys) by validation using a recommended pattern of ROC curves. Additionally, it was noted that the active ligands from the highest-ranked compounds in the database were closely observed by the designed pattern. The AUC curve was found to be 0.705 and the top 1% (6.25), a reliable enrichment factor (Fig. 8). The

sensitivity and specificity association is the ROC curve. It displays, on the y- and x-axes, the true positive and false positive fractions, appropriately[64].

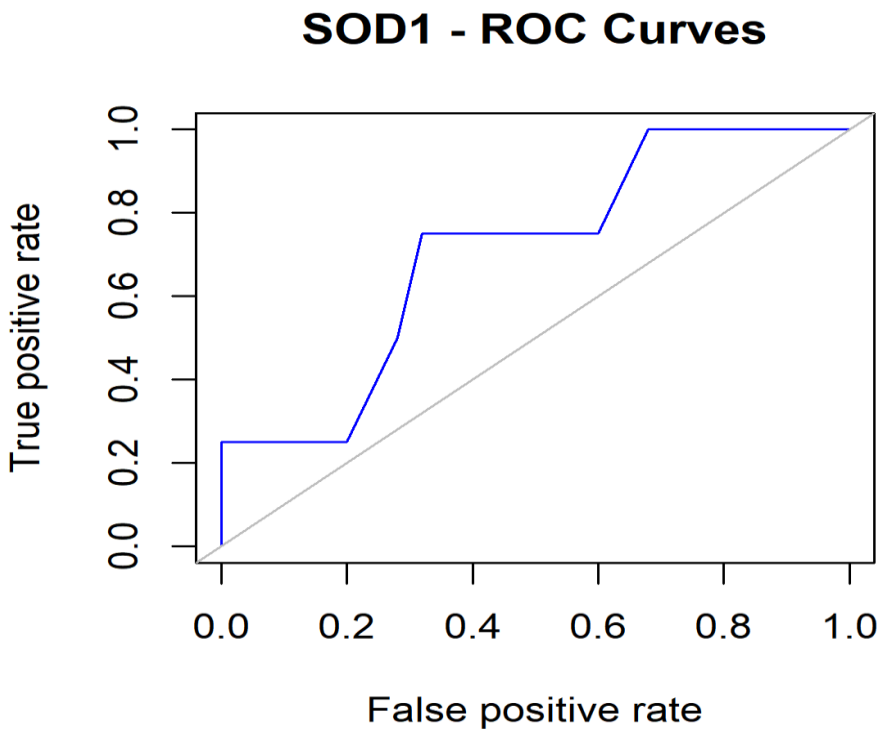


Figure 8: ROC curves of docking validation score

Molecular dynamics simulation analysis

The MD analyses of optimal chemical compounds with the protein target were performed for 100 ns. The trajectory of Desmond's analysis. Through MD trajectory analysis the values of RMSD and RMSF were determined, as well as interactions of protein-ligands and secondary structure of protein elements distribution by residue index.

RMSD analysis

Fig. 9 shows the time-dependent variation in RMSD for C-alpha atoms in the protein-ligand bound revealing the stability of the complexes. The RMSD plot (Fig 9A) showed that the 4a7v-Scytonine complex stabilized at 5 ns. However, there was an increase in RMSD slightly of protein bound to ligand at 30 ns. Throughout the simulation duration, the RMSD remains in the variation of 0.5 ns, which is fine. In the whole duration period of the simulation, there were no clear changes observed in ligand fit to protein. At 5 ns ligand gained equilibrium, there was no obvious fluctuation and the ligand remained tightly in the pocket of protein. The complexed 4a7v-Raocyclamide_A protein stabilized from the initial simulation according to the RMSD plot. The RMSD of protein at 50ns slightly fluctuates after that gained equilibrium through the whole duration of the simulation period. There was a slight flip in the RMSD graph of ligand at 30 ns due change in the conformation present of rotatory bonds of ligand. In (fig 9B) 2D representation of a ligand is shown which has rotatory bonds. These types of flips are caused by torsion angle in the ligand[65]. Once stability was achieved the RMSD of the ligand remained within the range of 0.5 Angstrom bound fit to protein, after equilibrium was attained, there was no variation in the RMSD of the ligand[66].

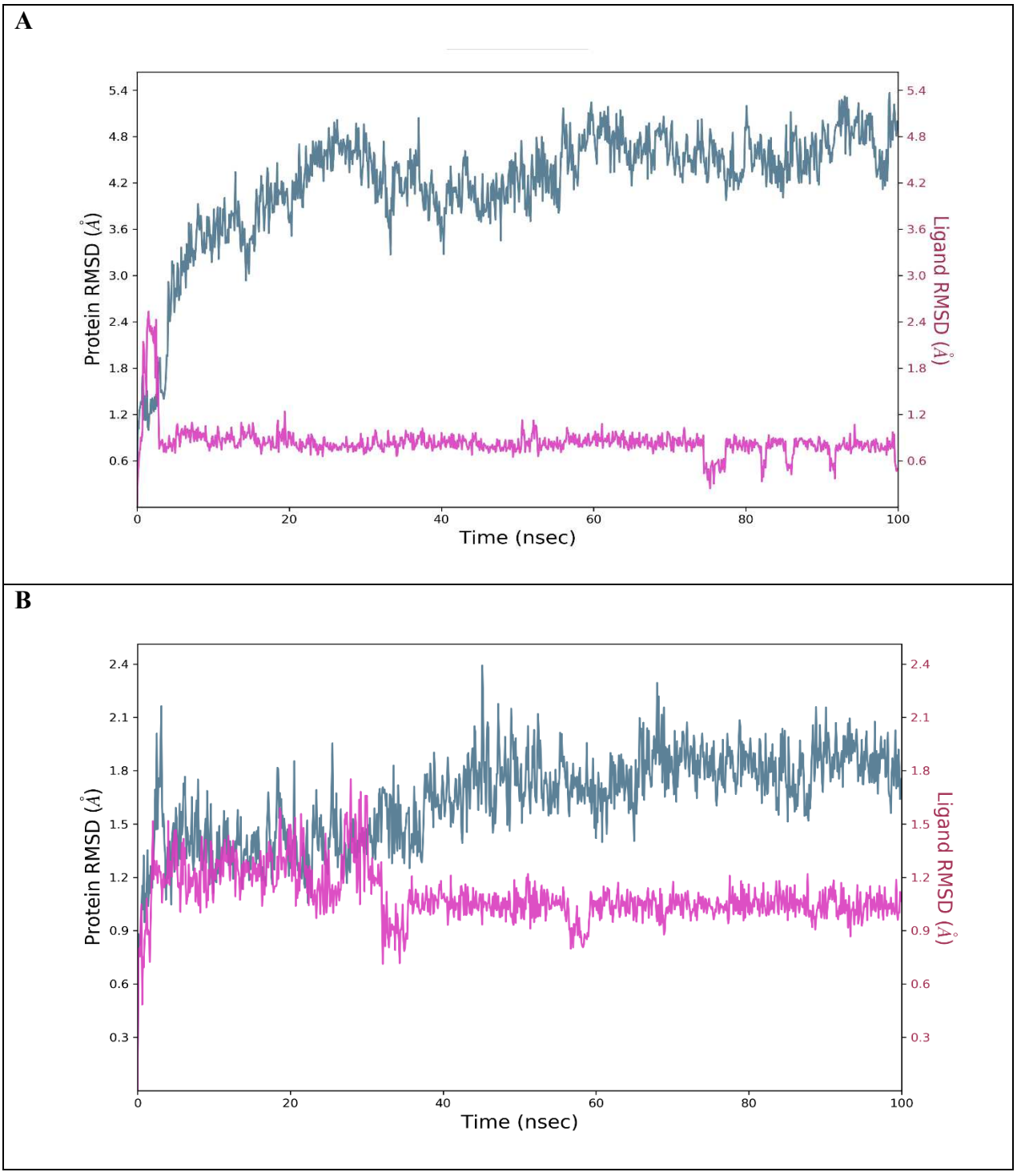


Figure 9: The variation in the (RMSD) root mean square deviation between the C-alpha atoms of the complexes (A: 4a7v-Scytonine and B: 4a7v-Raocyclamide_A) over time. The pink color shows the RMSD of the lead compounds and gray shows the RMSD of the protein.

RMSF analysis

The RMSF calculates the movement of each residue in the coupled protein-ligand complex. The dynamic behavior of protein-ligand complex were determined residue by residue in physiochemical situation through RMSF. In Figure 10, the value of RMSF protein-ligand complexes is shown. Some residues have higher peak values of RMSF due to flexible regions like loop coiling or the protein's N- and C-terminus ends. The residues in contact with ligand have lower peaks in RMSF value. The stability of complex proteins and ligands is associated with the RMSF values of these residues in the binding site of the ligand. The minimum fluctuation in protein-ligand complexes interaction decreases the RMSF for these binding site residues during the simulation period.

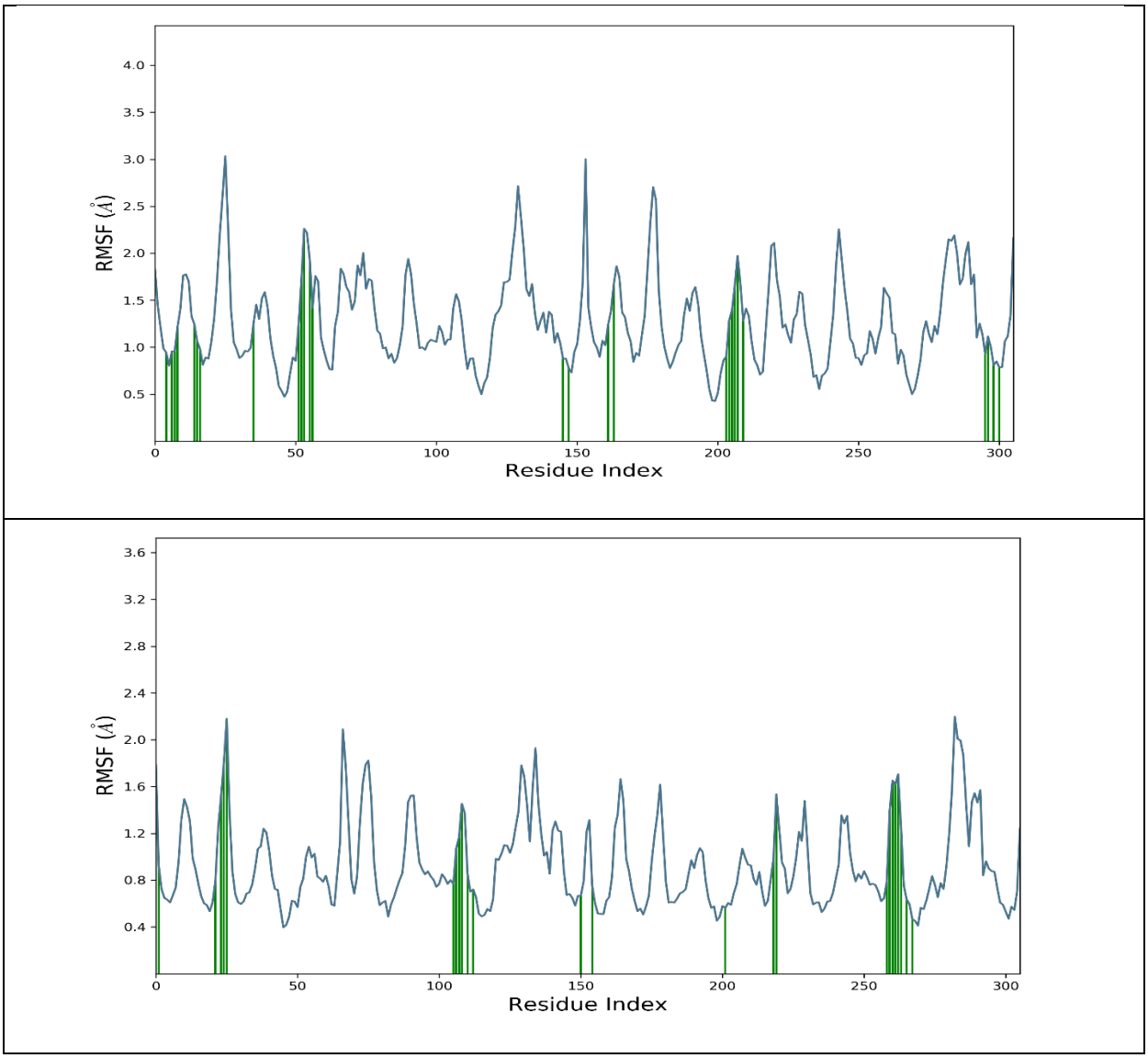


Figure 10: The RMSF Root Mean Square Fluctuation value of protein in ligand in term of residues. A: 4a7v-Scytonine, B: 4a7v-Raocyclamide_A.

Secondary structure elements

The features of secondary structure were tracked by analyzing alpha helices and beta-strands through simulation duration. The distribution of the protein structure was identified by plotting the Secondary Structure Elements chart against the residual index. It was noticed in the complex of 4a7v-Scytonine shown in (fig 11A) the total 36.58%, helix 0.91% and 35.67% made in secondary structure elements. It was observed in 4a7v-Raocyclamide_A that alpha-helices percentage 0.71%, beta-strands 36.17% and total percentage 36.88% in SSE plot (fig 11B). The ratio of alpha helices

and beta strands affect the deviation in complex. The lower RMSD appeared in rigid structure of protein as contracted in loops and coil region residues [67, 68]. The hydrogen bonds and hydrophobic interactions of 4a7v-Scytonine complex account for the vast majority of the important protein-ligand connection identify by MD.

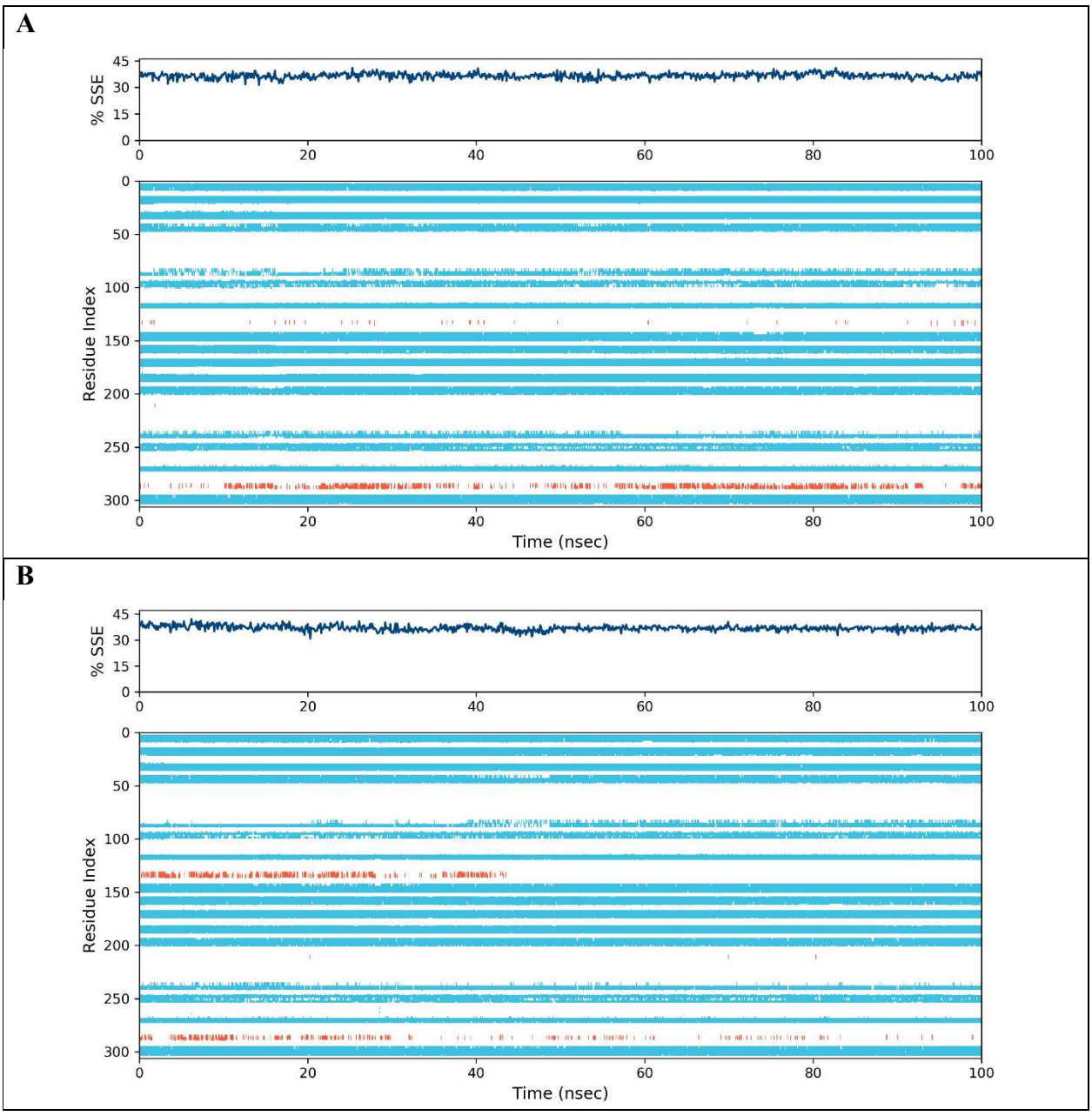


Figure 11: Elements of protein secondary structure with respect to residue index are dispersed across protein-ligand complexes. The alpha helices are represented by the red colors and the beta strands by the blue ones.

According to (Fig 12A) the hydrogen boning observed for LYS:F_9, ASP:F-11, ASN:A_53 and ASN:F_53 residue. For hydrophobic VAL:A_7, LYS:A_9, VAL:A_148 and VAL:A_148. In Figure 11B for 4a7v-Raocyclamide_A, the critical hydrogen residues observed by MD trajectory were LEU:A_106, SER:A_107, GLY:F_108 and ASP:F_109, for the interaction of hydrophobic ALA:A_1 and ILE:A_151 crucial amino acids residue. In Figure 12 the timeline charts of protein and ligand contacts are visualized, the timeline displays the contacts and interactions (H-bonds, hydrophobic, ionic, and water bridges). In a given panel at the top numbers of interaction count and at the bottom in each frame of the trajectory the interacting residues with ligand. The independent interaction of some residue with the ligand is shown in darker orange[69].

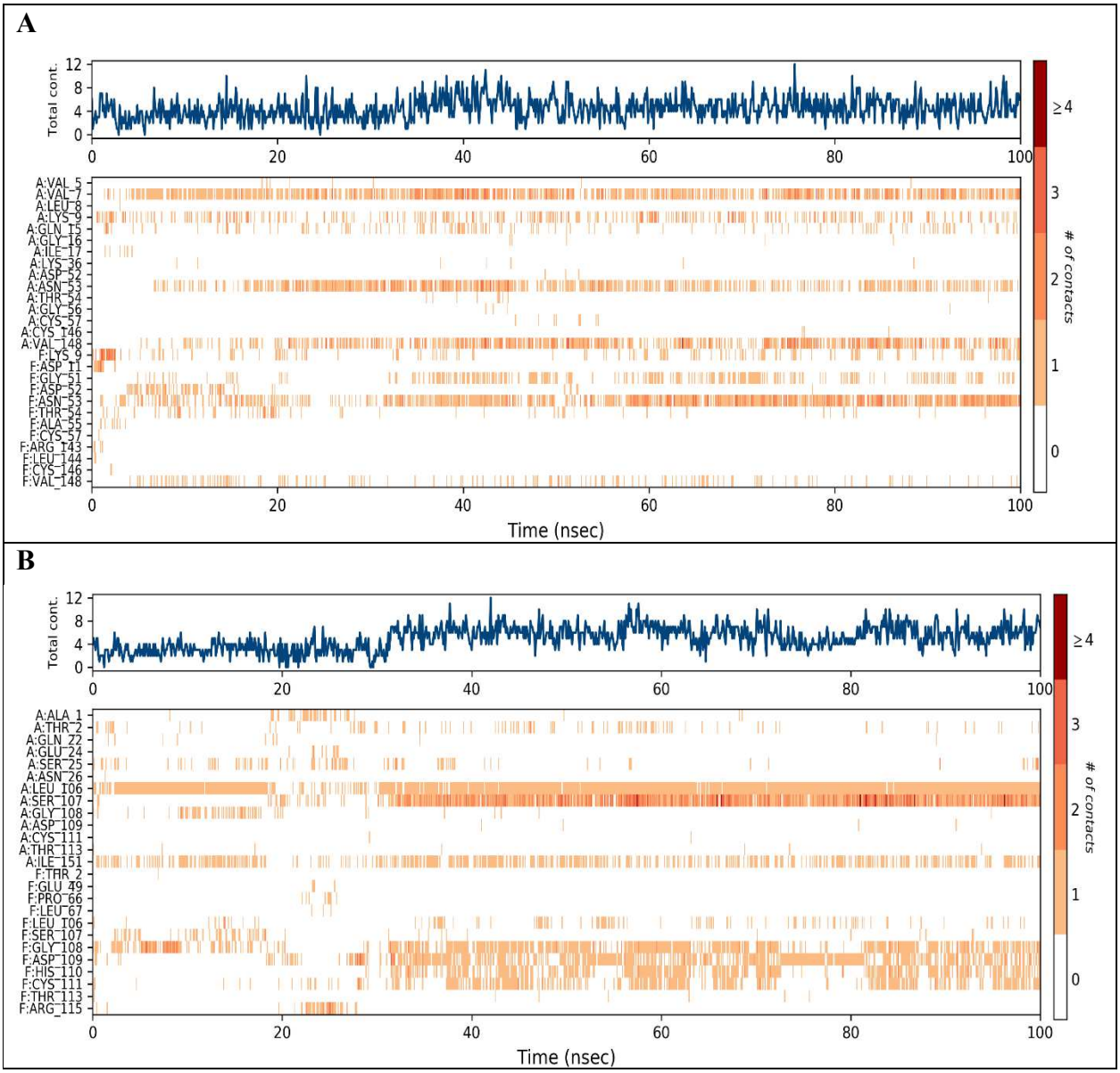


Figure 12: Protein-ligand contact heatmap throughout trajectory

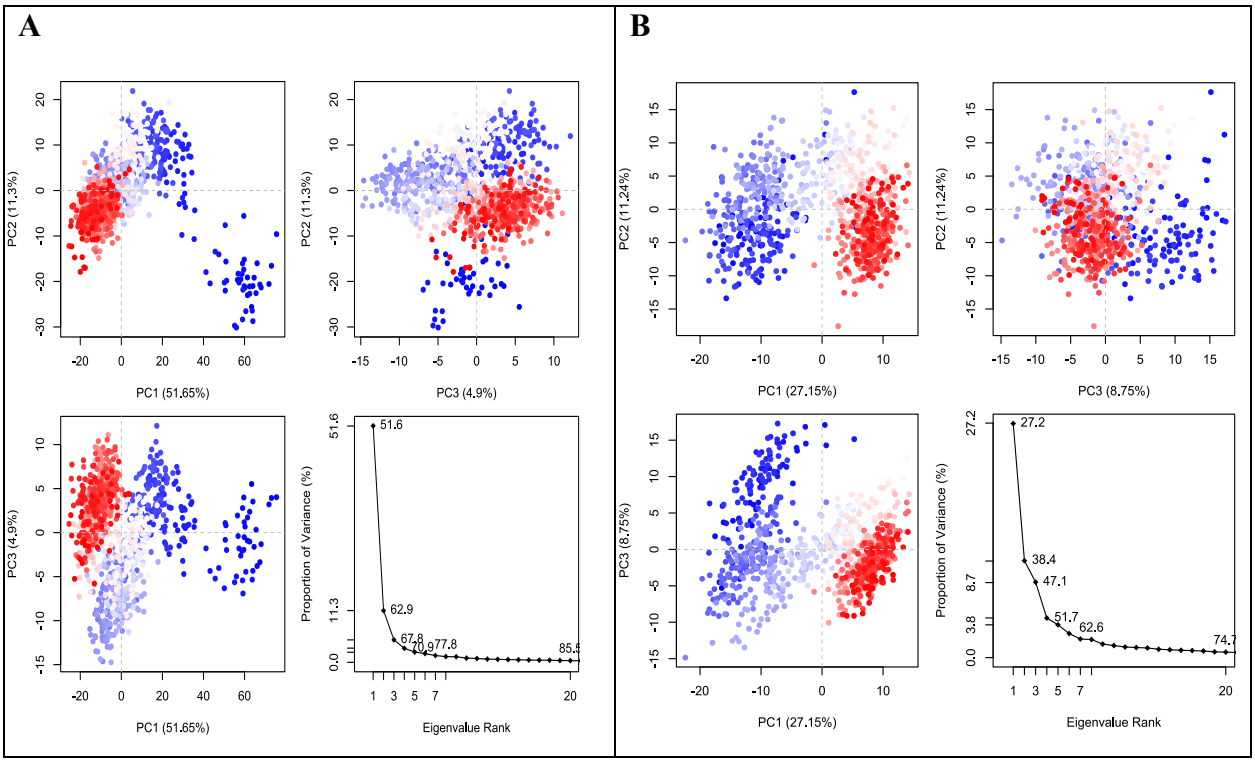


Figure 13: Plotting the principal component analysis eigenvalue against the variance percentage (A) 4a7v-Scytonine (B) 4a7v- Raocyclamide_A

Principal Component Analysis (PCA) describes the dynamics of proteins [70]. Calculations were made on the trajectory motions observed during MD simulations. The stability was demonstrated in the first 20 modes of motion (4a7v-Scytonine) (Fig. 13A) and (4a7v-Raocyclamide_A) (Fig. 13B) by plotting the eigenvalues (protein) against the eigenmode (eigenvector index). Eigenvalues span the hyperspace apparent eigenvector fluctuations. The target protein's overall mobility is regulated by eigenvectors with higher eigenvalues in simulated analyses. In 4a7v-Scytonine and 4a7v-Raocyclamide_A complexes, compared to the other eigenvectors, the top five eigenvectors in the used systems displayed dominant motions and had higher eigenvalues (51.6–77.8 %) and (27.2–62.6 %) respectively. On three PCs (PC1, PC2, and PC3), all changes were noted and visualized. For In 4a7v-Scytonine complex, the most variable PC1 clusters (51.65%), PC2 clusters (11.3%), and least variable PC3 clusters (4.9%) (Fig.13A) and in 4a7v-Raocyclamide_A complex, the PC1 clusters exhibited the highest variability (27.15%), followed by PC2 (11.924%), and PC3 (8.75%), which showed the least variability (Fig. 13B). PC3 has a more miniature structure than PC1 and PC2, and because of its low variability, it thought more stable protein ligand-binding complexes. Simple PC subspace clustering showed that all of the groups' conformations varied.

The blue color shows the greatest mobility, followed by white for moderate mobility and red for less flexibility[71].

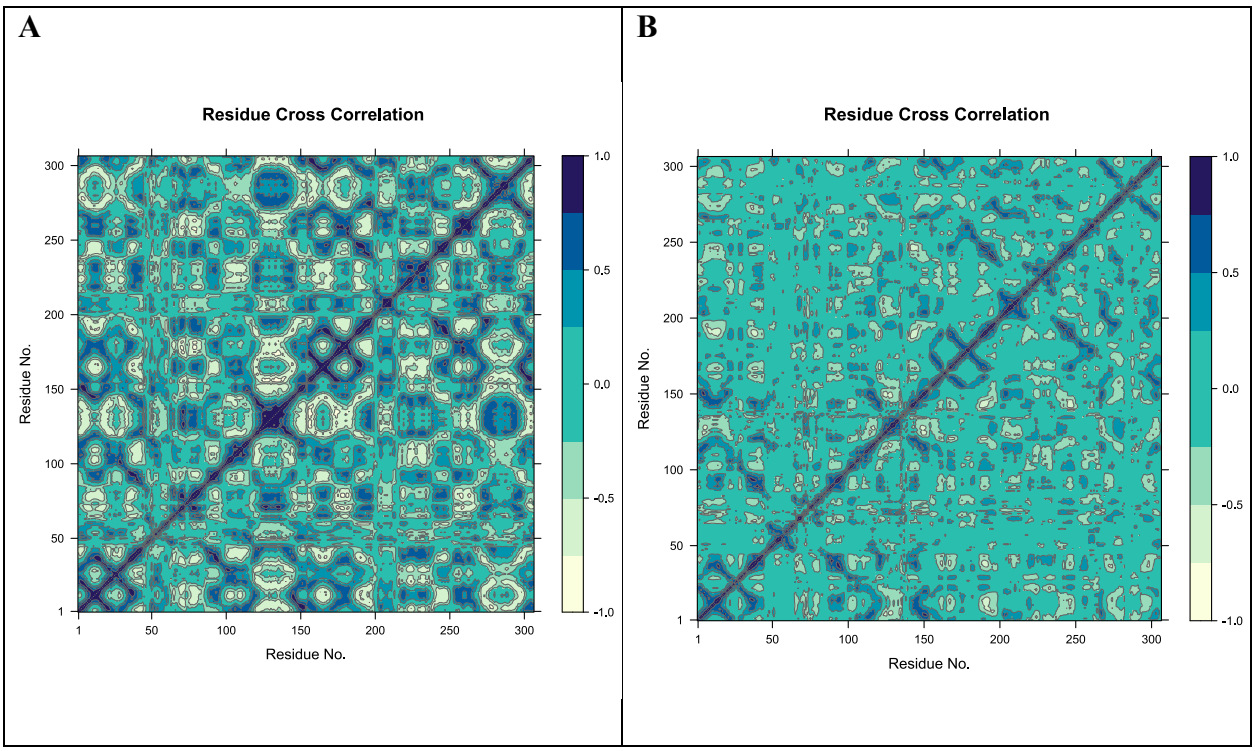


Figure 14: Figure 11. Intricate dynamic cross-correlation map. The purple and cyan colors respectively, represent the residues' positive and negative correlations. (A) 4a7v-Scytonine (B) 4a7v- Raocyclamide_A

The cross-correlation map indicated a strong association between the SOD1 target protein (4a7v) and the chosen ligands (Scytonine and Raocyclamide_A) based on the high pairwise cross-correlation coefficient value (Fig.14). The residues anti-correlated (-0.4) are represented by the color magenta, while residues correlated (>0.8) are represented by the color cyan. The high number of residues between the target protein (4a7v) and particular ligands that were found to be pairwise associated [72].

MMGBSA analysis

The MM-GBSA method is one approach that is widely used to assess the energy of interaction between drugs and the molecules of protein[73]. In addition to the binding free energy of the complex, it allows for the examination of other non-bonded interacting energies. A binding energy estimate of -47.66166668 kcal/mol was calculated for the Scytonine-4a7v and -48.79594608 kcal/mol for Raocyclamide_A with 4a7v interactions. As can be seen from Tables 4 and 5, non-bonded interactions like GbindCoulomb, GbindLipo, GbindHbond, GbindvdW, and GbindPacking regulate Gbind. Complete MM-GBSA results are shown in supplementary file S2.

Table 4. The MM-GBSA Calculation of Binding energy of Scytonine with 4a7v from MD simulation trajectories performed every 10 ns.

4a7v-Scytonine	dG_{bind}	$dG_{bind}Lipo$	$dG_{bind}vdW$	$dG_{bind}H_{bond}$	$dG_{bind}Packing$
0 ns	-46.43086496	-8.351332345	-47.45706635	-1.39713073	-0.10907136
10 ns	-36.92837681	-11.69960193	-46.51658209	-0.03779813	-2.716398283
20 ns	-38.57656181	-10.86260214	-47.52425128	-0.019006779	-3.819972565
30 ns	-41.37960325	-11.2387613	-50.816236	-0.457918817	-5.39685474
40 ns	-53.96011136	-13.65026675	-55.95478585	-0.557777094	-5.124684465
50 ns	-41.81281233	-12.12931632	-45.2314544	-0.173809193	-1.930432039
60 ns	-45.1916267	-12.83241736	-52.38230674	-0.010602785	-3.177588857
70 ns	-54.75442154	-14.76358302	-57.98885582	-0.111912982	-3.522406264
80 ns	-52.78426129	-13.58630591	-53.62886078	-0.03621788	-2.568897172
90 ns	-55.21644419	-14.67000944	-55.496831	-0.02688948	-3.835761992
100 ns	-57.24324919	-13.88420909	-56.35221714	-0.065851711	-3.550694778

The contributions of the GbindLipo, GbindvdW, and GbindCoulomb energies throughout a range of interaction types are reflected in typical binding energy. Conversely, GbindCovalent and GbindSolvGB energies influence average binding energies significantly. Additionally, the complexes 4a7v-Scytonine and 4a7v-Raocyclamide_A establish stable hydrogen bonds with the amino acid residues as shown by the dGbindHbond association values of the residues. Given this, the binding energy determined from the docking data agrees well with the results of MM-GBSA computations with MD simulation trajectories[74].

Table 5. The MM-GBSA Calculation of Binding energy of Raocyclamide_A with 4a7v from MD simulation trajectories performed every 10 ns.

4a7v-Scytonine	dG_{bind}	dG_{bind}Lipo	dG_{bind}vdW	$dG_{bind}H_{bond}$	dG_{bind}Packing
0 ns	-48.38066387	-12.06292829	-41.70867784	-1.806994563	-0.021003657
10 ns	-50.45523893	-9.587605997	-36.37493884	-1.683552975	-0.000267739
20 ns	-37.9610093	-9.718806934	-31.00940337	-1.067892979	-0.066874008
30 ns	-33.81308884	-8.501593419	-32.0898327	-0.79382447	-0.474646218
40 ns	-43.54203754	-11.56313597	-41.2202786	-0.854512212	-0.256610959
50 ns	-47.38124397	-13.89355653	-40.60300059	-1.00540847	-0.17181103
60 ns	-58.65417864	-14.06858828	-47.15097287	-1.157342958	-0.20938241
70 ns	-58.28402743	-13.56798011	-43.11010925	-1.007785359	-0.418913029
80 ns	-68.77725685	-14.44471973	-45.93270842	-1.320650066	-0.006066586
90 ns	-49.86928401	-12.88496505	-42.25114799	-1.269741458	-0.51357861
100 ns	-39.63737754	-13.28852016	-45.83394883	-1.371664838	-0.001318274

Discussion

About two to seven percent of sporadic ALS cases and 20% of all familial ALS cases are caused by mutation in SOD1. Numerous medicinal techniques are now being development, but only riluzole[75], an FDA-approved medication that lessens sickness. Since they have been demonstrated to be efficient therapies for thousands of years, natural substances and their analogues from diverse sources are used extensively in the treatment of a range of neurological disorders because of their neuro-pharmacological properties like anti-inflammatory and antioxidant[76]. The focus of this study was to offer a superior therapeutics that may function as an ALS disease inhibitor to the modern world. These investigations have added credence to the idea that ALS-causing protein SOD1 may be therapeutically targeted.

The process of creating new medications takes a lot of time, money, and interdisciplinary cooperation, but throughout the past 20 years, scientific developments have altered how the pharmaceutical industry yields new bioactive chemicals[77]. CADD approaches are therefore widely used nowadays to increase the efficacy of the drug research and development process. The fields of drug discovery and development recognize the effectiveness and potency of molecular docking, dynamics modeling, structure and ligand-based design of drug methodologies[78]. It is now much easier to understand the behavior and the structure of binding an exact ligand with a particular target molecule with the application of the CADD approach. At various stages of drug development, software and computational tools are becoming increasingly important in the field of pharmaceutical methods[79]. One effective method for locating the lead molecules in a chemical library is virtual screening. The structure-based medication design strategy was used in the current work, and a high throughput screening procedure was carried out utilizing a library of natural products that included 25,989 molecules. On the basis of RMSD score of pharmacophores, over 50 hits were kept. Additionally, ADMET and molecular docking study were performed on the compounds that demonstrated pharmacophore features in order to determine their binding affinity with the target SOD1 protein.

The majority of the compounds are dropouts of the lead molecules in the preclinical investigation because of their poor pharmacokinetics metrics and toxicity properties. As a result, using in silico approaches to estimate pharmacokinetics and toxicity compliances is essential. Molecular weight of all selected 130 to 725 grams per mole based on calculation[80]. Keep in view of binding

affinity, ADMET calculations and binding energy values of top compounds (Table 2), these analyses revealed that analyzed compounds showed particular biological properties. To share electrons to water molecules hydrogen bonds donors were calculated. Furthermore, a hydrogen bond acceptor is the approximate amount of hydrogen bonds that a solute found in water in aqua solutions will accept. The recommended range of non-integer values was observed from 0.0–6.0 for hydrogen bond donor and acceptor. The values that were determined were the average of multiple configurations. The values were computed by averaging values from several states that used in analyses, which resulted in non-integers and ranged from 2.0 to 20.0. The blockage of channels HERG K+ as the concentration of inhibitory values ((IC50) was calculated in between from -2.0 to 6.5. The calculation values of cell permeability prediction (Caco2) declared reliable and also by Caco2 cells the gut-blood barrier was examined. In addition, the values from zero to 25 consider poor and >500 considered as reliable. In the case of dopamine and serotonin, which have prognosticated ranges of 3.0 to 1.2 when using QikProp to identify the oral drugs are CNS-negative because to pass the blood-brain barrier because they are too polar. Predictions for QPlogKhsa and human serum albumin binding values from -1.5 to 1.5[81].

The purpose of the research involved is to find effective medicinal products approaches that target the SOD1 protein to treat the neurological condition ALS. In order to perform molecular docking studies with the target SOD1 protein, compounds that were devoid of ADMET analysis violations were chosen. Following an analysis of the drug kinetics and toxicological characteristics of the recovered natural chemicals, this specific option was selected[82]. Two compounds Scytonine and Raocyclamide_A that were chosen were found to have a higher binding propensity towards the target protein SOD1. Their respective docking values are -8.2 kcal/mol for scytonine and -8.2 kcal/mol for raocyclamide_A. The process of molecular docking was validated by ROC curve. An excellent area under the ROC of 0.705 represents that the docking tool notably improves docking accuracy with the target protein SOD1 and compounds[83].

Additionally, after evaluating the outcomes of the docking analysis, the top possible chemicals CID:10256051 (Scytonine) and CID:139586607 (Raocyclamide_A) were chosen for MD simulation studies. Throughout the simulation period, the SOD1 protein was shown to be stable with the chemicals CID:10256051 (scytonine) and CID:139586607 (raocyclamide_A). The RMSD analysis was used to evaluate the structural differences of the identified inhibitors with the

SOD1 target. The compounds are CID:139586607 (raocyclamide_A) and CID:10256051 (scytonine) revealed constant RMSD with average thresholds of 0.84 and 1.094 Å, respectively (Fig. 9). These results demonstrated the inhibitors' strong binding and overall stability inside the SOD1 binding region[84]. To understand the effects of the discovered inhibitors' binding on structure fluctuation of the SOD1 protein, the RMSF of the Cα atoms was assessed. The 4a7v-Scytonine and 4a7v-Raocyclamide_A complexes showed average RMSF values of 1.27 and 0.92 Å, respectively, as shown in Figure 10. According to the present results, the ligand and protein structures stayed mostly constant. RMSF and RMSD both showed local variation and stability.

In order to preserve the important information during simulation, PCA was utilized to reduce the dimensionality, and DCCM methods were applied for correlated and anti-correlated movements in complicated. The chemicals that demonstrated the highest levels of stability and binding in the physiochemical environment were remarkable. The reported ligands Scytonine and Raocyclamide_A has shown strong effectiveness against the targeted mutant SOD1 receptor through analyzing computational approaches and it may be these promising therapeutic drugs to treat amyotrophic lateral sclerosis disease with less side effects and more privilege outcomes. The reported compounds manifested least binding energy and higher efficient characteristics. Molecular docking and MD simulation analyses revealed that systematized ligand must have strong binding affinity, legitimate ADMET features and least binding energy[85]. In the light of selected extensive Insilco parameters that was proposed that Scytonine and Raocyclamide_A are potent drug molecules.

However, more research and thorough clinical studies are required to evaluate and confirm the results, adding to the body of knowledge already available on these substances and their possible use in the treatment of ALS. The development of effective treatments for ALS illness might be accelerated by these ongoing efforts, which could also improve patient outcomes overall.

Conclusion

In conclusion, the reported ligands Scytonine and Raocyclamide_A are strongly effective in amyotrophic lateral sclerosis by targeting mutant SOD1. Though detailed *in silico* analyses including molecular docking, ADMET and molecular dynamic analyses may be significant to conclude that Scytonine and Raocyclamide_A may be the potent therapeutic drug option for amyotrophic lateral sclerosis disease by targeting mutant SOD1. Significant stabilization was shown by the energetical and structural analyses conducted during the dynamic simulations for the discovered natural compounds Scytonine and Raocyclamide_A complexed with target protein. These finding will be useful for researcher and might lead to development of novel medicine for the treatment of amyotrophic lateral sclerosis disease.

Funding: No Funding

Data availability: All data generated or analysed during this study are included in this published article and its supplementary information files, S1 and S2.

References

1. Mukherjee, S., et al., *History, Origin and Types of Neurological Disorders.*
2. Srinivasan, E. and R. Rajasekaran, *Incidence, prevalence and disability associated with neurological disorders in Italy between 1990 and 2019: an analysis based on the Global Burden of Disease Study 2019.* Journal of Molecular Neuroscience 15 May 2020. **70**: p. 1742–1770.
3. Ahamad, S., et al., *A molecular journey to check the conformational dynamics of tau tubulin kinase 2 mutations associated with Alzheimer's disease.* RSC Adv, 2021. **11**(3): p. 1320-1331.
4. Zehravi, M., et al., *A Prospective Viewpoint on Neurological Diseases and Their Biomarkers.*
5. Ahamad, S., I.T. Junaid, and D. Gupta, *Computational Design of Novel Tau-Tubulin Kinase 1 Inhibitors for Neurodegenerative Diseases.* Pharmaceuticals (Basel), 2024. **17**(7).
6. Valentine, J.S., *Do oxidatively modified proteins cause ALS?* Free Radical Biology and Medicine, 15 November 2002. **Volume 33**(Issue 10): p. Pages 1314-1320.
7. Alsultan, A.A., et al., *The genetics of amyotrophic lateral sclerosis: current insights.* Degener Neurol Neuromuscul Dis, 2016. **6**: p. 49-64.
8. Kaur, S.J., S.R. McKeown, and S. Rashid, *Mutant SOD1 mediated pathogenesis of Amyotrophic Lateral Sclerosis.* Gene, 2016. **577**(2): p. 109-18.
9. Canosa, A., et al., *Amyotrophic lateral sclerosis with SOD1 mutations shows distinct brain metabolic changes.* Eur J Nucl Med Mol Imaging, 2022. **49**(7): p. 2242-2250.
10. P Masrori, P.V.D., *Amyotrophic lateral sclerosis: a clinical review.* European journal of neurology.
11. Mathis, S., et al., *Genetics of amyotrophic lateral sclerosis: A review.* Journal of the Neurological Sciences, 15 April 2019. **Volume 399**: p. Pages 217-226.
12. Ingre, C., et al., *Risk factors for amyotrophic lateral sclerosis.* Clin Epidemiol, 2015. **7**: p. 181-93.
13. Yu, Y., et al., *Environmental risk factors and amyotrophic lateral sclerosis (ALS): a case-control study of ALS in Michigan.* PLoS One, 2014. **9**(6): p. e101186.
14. Furtado Bastos, A., et al., *Amyotrophic Lateral Sclerosis: One or Multiple Causes?*
15. Wright, G.S.A., et al., *Ligand binding and aggregation of pathogenic SOD1.* Nature Communications, 2013. **4**(1): p. 1758.
16. Wright, G.S., et al., *Ligand binding and aggregation of pathogenic SOD1.* Nat Commun, 2013. **4**: p. 1758.

17. Hayashi, Y., K. Homma, and H. Ichijo, *SOD1 in neurotoxicity and its controversial roles in SOD1 mutation-negative ALS.* Adv Biol Regul, 2016. **60**: p. 95-104.
18. Srinivasan, E. and R. Rajasekaran, *A Systematic and Comprehensive Review on Disease-Causing Genes in Amyotrophic Lateral Sclerosis.*
19. Kiernan, M.C., et al., *Amyotrophic lateral sclerosis.* Lancet, 2011. **377**(9769): p. 942-55.
20. Kiernan, M.C., et al., *Chapter Fifty-One - Nonmotor Symptoms in Amyotrophic Lateral Sclerosis: A Systematic Review.* International Review of Neurobiology, 2011. **377**(9769): p. 942-955.
21. Talbott, E.O., A.M. Malek, and D. Lacomis, *Chapter 13 - The epidemiology of amyotrophic lateral sclerosis.* Handbook of Clinical Neurology, 2016. **Volume 138**: p. Pages 225-238.
22. Hardiman, O., *Management of respiratory symptoms in ALS.*
23. Gordon, P.H., et al., *Predicting survival of patients with amyotrophic lateral sclerosis at presentation: a 15-year experience.* Neurodegener Dis, 2013. **12**(2): p. 81-90.
24. Hobson, E.V. and C.J. McDermott, *Supportive and symptomatic management of amyotrophic lateral sclerosis.*
25. de Carvalho, M., et al., *Electrodiagnostic criteria for diagnosis of ALS.* Clin Neurophysiol, 2008. **119**(3): p. 497-503.
26. Ferguson, T.A. and L.B. Elman, *Clinical presentation and diagnosis of Amyotrophic Lateral Sclerosis.*
27. Goutman, S.A., et al., *Recent advances in the diagnosis and prognosis of amyotrophic lateral sclerosis.* Lancet Neurol, 2022. **21**(5): p. 480-493.
28. Ahamad, S., K. Hema, and D. Gupta, *Identification of Novel Tau-Tubulin Kinase 2 Inhibitors Using Computational Approaches.* ACS Omega, 2023. **8**(14): p. 13026-13037.
29. Ahamad, S., et al., *The structural, functional, and dynamic effect of Tau tubulin kinase1 upon a mutation: A neuro-degenerative hotspot.* J Cell Biochem, 2021. **122**(11): p. 1653-1664.
30. Pathak, R.K., et al., *Computational Approaches in Drug Discovery and Design.*
31. Prieto-Martínez, F.D., et al., *Chapter 2 - Computational Drug Design Methods—Current and Future Perspectives.* In Silico Drug Design Repurposing Techniques and Methodologies, 2019: p. 19-44.
32. Kingston, D.G.I., *Modern Natural Products Drug Discovery and Its Relevance to Biodiversity Conservation.* Journal of Natural Products, 2011.
33. Rishton, G.M., *Natural products as a robust source of new drugs and drug leads: past successes and present day issues.* The American journal of cardiology, 2008. **101**(10): p. S43-S49.
34. Lahlou, M., *The success of natural products in drug discovery.* 2013.
35. Berman, H.M., et al., *The Protein Data Bank.* Nucleic Acids Res, 2000. **28**(1): p. 235-42.
36. Eswar, N., et al., *Comparative protein structure modeling using Modeller.* Curr Protoc Bioinformatics, 2006. **Chapter 5**: p. Unit-5 6.
37. Ho, B.K. and R. Brasseur, *The Ramachandran plots of glycine and pre-proline.* BMC Struct Biol, 2005. **5**: p. 14.
38. Guex, N. and M.C. Peitsch, *SWISS-MODEL and the Swiss-PdbViewer: an environment for comparative protein modeling.* Electrophoresis, 1997. **18**(15): p. 2714-23.
39. Tian, W., et al., *CASTp 3.0: computed atlas of surface topography of proteins.* Nucleic Acids Res, 2018. **46**(W1): p. W363-w367.

40. van Santen, J.A., et al., *The Natural Products Atlas 2.0: a database of microbially-derived natural products.* Nucleic Acids Research, 2022. **50**(D1): p. D1317-D1323.
41. Sunseri, J. and D.R. Koes, *Pharmit: interactive exploration of chemical space.* Nucleic Acids Res, 2016. **44**(W1): p. W442-8.
42. Koes, D.R., *The Pharmit Backend: A Computer Systems Approach to Enabling Interactive Online Drug Discovery.* IBM J Res Dev, 2018. **62**(6): p. 1-6.
43. Yadav, S., et al., *Lead optimization, pharmacophore development and scaffold design of protein kinase CK2 inhibitors as potential COVID-19 therapeutics.* J Biomol Struct Dyn, 2023. **41**(5): p. 1811-1827.
44. Shiri, F., S. Pirhadi, and A. Rahmani, *Identification of new potential HIV-1 reverse transcriptase inhibitors by QSAR modeling and structure-based virtual screening.* J Recept Signal Transduct Res, 2018. **38**(1): p. 37-47.
45. Trott, O. and A.J. Olson, *AutoDock Vina: improving the speed and accuracy of docking with a new scoring function, efficient optimization, and multithreading.* J Comput Chem, 2010. **31**(2): p. 455-61.
46. Mura, C., et al., *An introduction to biomolecular graphics.* PLoS Comput Biol, 2010. **6**(8).
47. Mysinger, M.M., et al., *Directory of useful decoys, enhanced (DUD-E): better ligands and decoys for better benchmarking.* J Med Chem, 2012. **55**(14): p. 6582-94.
48. Empereur-Mot, C., et al., *Predictiveness curves in virtual screening.* J Cheminform, 2015. **7**: p. 52.
49. S.R., C., *How to calculate ROC curves.* 2013.
50. Ligprep, M. and G. Macromodel, *QikProp; Schrodinger, LLC; New York, NY, 2011*.
51. Bowers, K.J., et al. *Scalable algorithms for molecular dynamics simulations on commodity clusters*. in *Proceedings of the 2006 ACM/IEEE Conference on Supercomputing*. 2006.
52. Ferreira, L.G., et al., *Molecular docking and structure-based drug design strategies.* Molecules, 2015. **20**(7): p. 13384-421.
53. Hildebrand, P.W., A.S. Rose, and J.K.S. Tiemann, *Bringing Molecular Dynamics Simulation Data into View.* Trends Biochem Sci, 2019. **44**(11): p. 902-913.
54. Shivakumar, D., et al., *Prediction of Absolute Solvation Free Energies using Molecular Dynamics Free Energy Perturbation and the OPLS Force Field.* J Chem Theory Comput, 2010. **6**(5): p. 1509-19.
55. Alsukaibi, A.K.D., et al., *Chemical, biological and in silico assessment of date (P. dactylifera L.) fruits grown in Ha'il region.* Front Chem, 2023. **11**: p. 1138057.
56. Jha, A.N., G.K. Ananthasuresh, and S. Vishveshwara, *A search for energy minimized sequences of proteins.* PLoS One, 2009. **4**(8): p. e6684.
57. Sahinidis, N.V., *Optimization techniques in molecular structure and function elucidation.* Comput Chem Eng, 2009. **33**(12): p. 2055-2062.
58. Mannige, R.V., J. Kundu, and S. Whitelam, *The Ramachandran Number: An Order Parameter for Protein Geometry.* PLoS One, 2016. **11**(8): p. e0160023.
59. Li, C., et al., *Recent progress in drug delivery.* Acta pharmaceutica sinica B, 2019. **9**(6): p. 1145-1162.
60. Eberhardt, J., et al., *AutoDock Vina 1.2.0: New Docking Methods, Expanded Force Field, and Python Bindings.* J Chem Inf Model, 2021. **61**(8): p. 3891-3898.

61. Norinder, U. and C.A. Bergstrom, *Prediction of ADMET Properties.* ChemMedChem, 2006. **1**(9): p. 920-37.
62. Bultel-Ponce, V., et al., *New pigments from the terrestrial cyanobacterium Scytonema sp. collected on the Mitaraka inselberg, French Guyana.* J Nat Prod, 2004. **67**(4): p. 678-81.
63. Admi, V., U. Afek, and S. Carmeli, *Raocyclamides A and B, Novel Cyclic Hexapeptides Isolated from the Cyanobacterium Oscillatoria raoi.* Journal of Natural Products, 1996. **59**(4): p. 396-399.
64. Safari, S., et al., *Evidence Based Emergency Medicine; Part 5 Receiver Operating Curve and Area under the Curve.* Emerg (Tehran), 2016. **4**(2): p. 111-3.
65. Hao, M.H., O. Haq, and I. Muegge, *Torsion angle preference and energetics of small-molecule ligands bound to proteins.* J Chem Inf Model, 2007. **47**(6): p. 2242-52.
66. Hollingsworth, S.A. and R.O. Dror, *Molecular Dynamics Simulation for All.* Neuron, 2018. **99**(6): p. 1129-1143.
67. Zhang, G. and Z. Su, *Inferences from structural comparison: flexibility, secondary structure wobble and sequence alignment optimization.* BMC Bioinformatics, 2012. **13 Suppl 15**(Suppl 15): p. S12.
68. Carugo, O. and S. Pongor, *A normalized root-mean-square distance for comparing protein three-dimensional structures.* Protein Sci, 2001. **10**(7): p. 1470-3.
69. Corradi, V., et al., *Emerging Diversity in Lipid-Protein Interactions.* Chem Rev, 2019. **119**(9): p. 5775-5848.
70. David, C.C. and D.J. Jacobs, *Principal Component Analysis: A Method for Determining the Essential Dynamics of Proteins*, in *Protein Dynamics: Methods and Protocols*, D.R. Livesay, Editor. 2014, Humana Press: Totowa, NJ. p. 193-226.
71. Ashraf, N., et al., *Combined 3D-QSAR, molecular docking and dynamics simulations studies to model and design TTK inhibitors.* Frontiers in Chemistry, 2022. **10**.
72. Yousaf, N., et al., *Exploiting the co-crystal ligands shape, features and structure-based approaches for identification of SARS-CoV-2 Mpro inhibitors.* Journal of Biomolecular Structure and Dynamics, 2023. **41**(23): p. 14325-14338.
73. Godschalk, F., et al., *Comparison of MM/GBSA calculations based on explicit and implicit solvent simulations.* Physical Chemistry Chemical Physics, 2013. **15**(20): p. 7731-7739.
74. Decherchi, S. and A. Cavalli, *Thermodynamics and Kinetics of Drug-Target Binding by Molecular Simulation.* Chemical Reviews, 2020. **120**(23): p. 12788-12833.
75. Saitoh, Y. and Y. Takahashi, *Riluzole for the treatment of amyotrophic lateral sclerosis.* Neurodegenerative disease management, 2020. **10**(6): p. 343-355.
76. Rehman, M.U., et al., *Neuroprotective strategies for neurological disorders by natural products: an update.* Current neuropharmacology, 2019. **17**(3): p. 247-267.
77. Psimadas, D., et al., *Molecular nanomedicine towards cancer: 111In-labeled nanoparticles.* Journal of pharmaceutical sciences, 2012. **101**(7): p. 2271-2280.
78. Surabhi, S. and B.K. Singh, *Computer aided drug design: an overview.* Journal of Drug delivery and Therapeutics, 2018. **8**(5): p. 504-509.
79. Usha, T., et al., *Recent updates on computer-aided drug discovery: time for a paradigm shift.* Current topics in medicinal chemistry, 2017. **17**(30): p. 3296-3307.
80. Release, S., *3: QikProp, Schrödinger, LLC, New York, NY, 2023*. 2023.
81. Ioakimidis, L., et al., *Benchmarking the reliability of QikProp. Correlation between experimental and predicted values.* 2008. **27**(4): p. 445-456.

82. Ibrahim, M.A.A., et al., *In silico drug discovery of SIRT2 inhibitors from natural source as anticancer agents.* Scientific Reports, 2023. **13**(1): p. 2146.
83. Yu, W. and A.D. MacKerell, Jr., *Computer-Aided Drug Design Methods.* Methods Mol Biol, 2017. **1520**: p. 85-106.
84. Ibrahim, M.A.A., et al. *In-Silico Mining of the Toxins Database (T3DB) towards Hunting Prospective Candidates as ABCB1 Inhibitors: Integrated Molecular Docking and Lipid Bilayer-Enhanced Molecular Dynamics Study*. Pharmaceuticals, 2023. **16**, DOI: 10.3390/ph16071019.
85. Abdeljawaad, K.A.A., et al., *Potential P-glycoprotein (P-gp) inhibitors from SuperDRUG2 database toward reversing multidrug resistance in cancer treatment: Database mining, molecular dynamics, and binding energy estimations.* J Mol Graph Model, 2025. **137**: p. 108997.

Supplementary Files

This is a list of supplementary files associated with this preprint. Click to download.

- S1.csv
- S2.csv